Volume 6, Issue 3, 2016, 1214-1221 ISSN 2069-5837

Biointerface Research in Applied Chemistry

www.BiointerfaceResearch.com

Original Research Article Open Access Journal

Received: 15.01.2016 / Revised: 25.02.2016 / Accepted: 28.03.2016 / Published on-line: 01.04.2016

Modeling the effect of autoreactive T-cells on oligodendrocytes in multiple sclerosis patients using chitosan/gelatin nanofibrous scaffolds

Amir Salati [1], Ghasem Ahangari [1], Hamid Keshvari [2], Mohammad Hossein Sanati [1,*]

[1]Department of Medical Biotechnology, National Institute of Genetic Engineering and Biotechnology, Tehran, Iran
[2]Department of Biomedical Engineering, Amirkabir University of Technology, Tehran, Iran

*corresponding author e-mail address: ***drmhsanati@yahoo.com***

ABSTRACT

In this study, nanofiberous scaffolds were fabricated from chitosan and gelatin at different blends (chitosan/gelatin: 80/20, 50/50, and 20/80) using electrospinning. Scanning electron microscopy (SEM), contact angle test, porosity measurement, and scaffold biocompatibility through PC-12 cells were used to evaluate scaffolds for tissue engineering applications. Nanofibers with 50% chitosan and 50% gelatin were the ideal option for neural tissue engineering. Thereafter, T-cells were obtained from peripheral blood of multiple sclerosis (MS) patients and healthy controls. In addition, the assessments of the effects of MS patients' T-cells on OLN-93 cells number and morphology were carried out onto optimal fabricated nanofibrous scaffold. Finally, mRNA analysis of oligodendrocytes was performed for the evaluation of B7-1(CD80), B7-2(CD86), and IL-12p40 expressions. The results showed that the expressions of these molecules in OLN-93 cells increased as expected. Also, the finding showed that the designed environment as an *in vitro* model for MS can be used for future studies on MS treatment.

Keywords: *Neural tissue engineering, multiple sclerosis, nanofibers, chitosan, gelatin.*

1. INTRODUCTION

Multiple sclerosis (MS) is one of the most common inflammatory and autoimmune diseases that destroy myelin-forming oligodendrocytes of the central nervous system (CNS) [1, 2]. Oligodendrocyte is responsible for manufacturing myelin in the CNS. Although, the etiology of MS remains unknown, there is an aggressive autoreactive T-cell attack on myelin as the main event in the pathogenesis of MS [3]. Previous studies have shown that there is a large variety of biomarkers in M [4, 5] and specially, B7-1 (CD80), B7-2 (CD86), and IL-12p40 are differently involved in T-cell stimulation [6-10]. Also, the upregulations of B7-1, B7-2, and IL-12 in MS are directly related to conditions that maximally stimulate T cell activation. These molecules were shown to be involved in T helper1 type and T helper 2-like responses [11, 12]. It is known that the CNS is complicated. Interaction of different cells with each other and immune-neurological interactions is one of the important parameters in this intricacy. For *in vitro* modeling of MS, it can be made less complex by using single type cells or mixed cell cultures [13]. But due to (1) primary cultures of rodent, CNS cells are often restricted to cells isolated from embryonic stages, particularly neurons and oligodendrocytes and (2) that fact that these cells are often difficult to obtain from adult animals, and more so from human tissues; therefore, transformed cells and cell lines are generally used. Among these cells, OLN-93 is a permanent oligodendroglial cell line derived from transformed cells in primary rat brain glial cultures [14]. In this study, attempt was made to apply tissue engineering techniques for assessment of T-cells effects on oligodendrocytes in MS patients. Although, the main goal of tissue engineering is providing new medical therapies using biomaterials and it recently developed an approach which plans to overcome the limitations of organ transplantation [15-18]. Tissue engineering has a high capacity for *in vitro* modeling of diseases, such as MS. The essential approach in tissue engineering involves the fabrication of scaffolds with cells to produce a functional tissue suitable for implantation. The main subject for tissue engineered scaffolds is manufacturing biodegradable matrices that can imitate the extracellular matrices (ECM) [18]. ECM plays a vital role in supporting and controlling cell behavior. For this reason, the scaffolds should be designed accordingly [19]. Nanofiberous scaffolds fabricated by electrospinning are applied as proper environment for cell attachment, and proliferation due to likeness to physical dimension of natural ECM [20-22]. Electrospinning is a method that utilizes electric force for producing polymer fibers from melts or solutions [23-25]. Polymer blending is an effective method for providing desirable scaffolds for neural tissue engineering applications. The properties of a biocomposite were influenced by the ratios of the added compounds that modified their biological properties for neurons viability and spreading [26-29]. A large number of polymers have been examined for providing excellent environment for neural tissue engineering applications. Among these polymers, natural polymers such as chitosan and gelatin do not cause foreign body response. They are both widely used biomaterials in nerve tissue engineering [30-36]. Chitosan can be blended with other polymers in organic solvent solutions to have excellent fiber-forming ability. Also, in the mixture of chitosan and gelatin, nanofiberous mats have a lot of desired properties for tissue engineering applications, but owing to their structural similarity to ECM, they have very large surface area and provide high porosity [37, 38]. This study was carried out to investigate the effects of MS patients T-cells on the morphology of OLN-93 cells and evaluation of mRNA analysis of OLN-93 cells by using chitosan and gelatin nanofiberous scaffolds. Therefore, first, chitosan and gelatin were

dissolved in an acetic acid solution. Next, gelatin–chitosan nanofibers were prepared by electrospinning. A crosslinking agent was used to stabilize nanofiberous scaffold. Then, biocompatibility of nanofiberous scaffold was determined by PC12 cells culture. Finally, for designing a simple *in vitro* model of MS, cell viability, spreading and morphology of OLN-93 cells in the presence of the T-cells were measured and also mRNA analysis of OLN-93 cells (seeded on the tissue-engineered scaffold) was done.

2. EXPERIMENTAL SECTION

2.1. Subjects.

Eight patients with relapsing-remitting MS (6 females and 2 males) and eight healthy controls (5 females and 3 males) were included in this study (Table 1). The median age of patients and controls was 35 years (range: 21 to 50 years) and 33 years (range: 22 to 45), respectively.

Table1. Eight patients with relapsing-remitting Multiple sclerosis (RRMS) and eight healthy controls were included in this study. The diagnosis was made based on magnetic resonance imaging examinations. NS: normal subjects. RRMS: relapsing-remitting multiple sclerosis.

Subject	Age/Sex	Disease duration (Years)	Type
MS-1	24/M	4	RRMS
MS-2	32/M	5	RRMS
MS-3	21/F	2	RRMS
MS-4	45/F	7	RRMS
MS-5	39/F	6	RRMS
MS-6	29/F	3	RRMS
MS-7	50/F	3	RRMS
MS-8	41/F	11	RRMS
NS-1	26/M	---	---
NS-2	45/M	---	---
NS-3	37/M	---	---
NS-4	31/F	---	---
NS-5	42/F	---	---
NS-6	33/F	---	---
NS-7	22/F	---	---
NS-8	31/F	---	---

2.2. Materials.

Gelatin, acetic acid and glutaraldehyde (GA) were purchased from Merck. Chitosan (degree of deacetylation 0.85, MW 110 kDa), Dulbecco's modified Eagle medium (DMEM), RPMI-1640 medium, penicillin/streptomycin, fetal calf serum (FCS), dimethyl sulfoxide (DMSO), horse serum (HS) and human AB serum were obtained from Sigma–Aldrich. Phosphate buffered saline (PBS), fetal bovine serum (FBS), TRIzol Reagent, Dynabeads Untouched Human CD4 T Cells kit, GlutaMAX I and 4-(2-hydroxyethyl)-1-piperazineethanesulfonic acid (HEPES) were received from Invitrogen. Reverse transcription System and Poly(A)-Tract mRNA isolation system were obtained from Promega and Lymphoprep was purchased from Nycom Pharma. All products were used without further purification.

2.3. Nanofiberous scaffolds preparation: Electrospinning.

Gelatin 30% (w/v) and chitosan 3% (w/v) were dissolved in 80% acetic acid and 20% deionized water solution. Then, the solutions were blended at the ratios of 80:20, 50:50, and 20:80 at room temperature with stirring for 20 h. Mats were fabricated by electrospinning machine. The blended biopolymers were fed into a 1 ml syringe. The diameter of nozzle was 0.1 mm. Also, the applied voltage, flow rate, and distance between the tip of the needle and collector were fixed at 12 kV, 0.1 ml/h, and 16 cm respectively in all experiments.

2.4. Crosslinking.

The crosslinking procedure was done by placing the chitosan-gelatin nanofiberous scaffolds in a sealed desiccator containing 10 ml of 25% glutaraldehyde aqueous solution in a Petri dish. The scaffolds were placed on a holed shelf in the desiccator and were crosslinked in an atmosphere of water and glutaraldehyde vapor at room temperature for 48 h. After crosslinking, the samples were exposed in the vacuum oven at room temperature.

2.5. Scanning electron microscopy (SEM).

By using SEM (KYKY EM-3200, China), the characterization of the nanofiberous scaffolds was determined. For samples preparation, a small section of the electrospun fiber was sputtered with a thin layer of gold prior to SEM observation. The SEM was carried out after sputter coating with gold at accelerating voltage of 24 kV. Cell morphology on nanofiberous scaffolds can be influenced by the fiber diameter; for this reason, fiber diameter was determined in different areas in each mat using the NIH ImageJ program. All data presented were the mean values of 10 measurements.

2.6. Contact angle and porosity measurement.

Water contact angles of nanofiberous scaffolds were measured using the sessile drop method employing a Kruss (Germany) G10 contact-angle measurement equipment. First, samples of the nanofiberous scaffolds were cut into square specimens with the size of 1 cm×1 cm, followed by placing them on a plate. Then, 5-µl distilled water droplet was used for each point and the contact angles between water droplets and the nanofiber mat specimens were determined using photos taken at various time periods (1, 5, 10, 30, and 60 s). Several measurements at different positions were carefully conducted for each specimen. The average values of five measurements on different points of each sample were recorded.

Porosity of the nanofiberous scaffolds were measured using mercury porosimeter (Micromeritics Instrument, Norcross, USA). The procedures of measurement and sample preparation were carried out according to the instructions provided by the manufacturer. Briefly, nanofiberous scaffolds with 500 µm thickness were cut into rectangular shapes (2×5 cm^2) and weighed. An electrospun scaffold was placed in the cup of the penetrometer, which was closed by tightening the cap. The penetrometer was sent into the pressure chamber of the porosimeter for assessment

of porosity. Equilibration time was 10 s and mercury filling pressure was 1.23 psia in this test.

2.7. Generation of T-cell lines.

Peripheral blood (10 ml) was obtained from each subject. Peripheral blood mononuclear cells (PBMC) isolation, cryopreservation and thawing were carried out as previously described [39]. PBMC isolation was performed by Lymphoprep. PBMCs were cryopreserved in heat-inactivated, filtered human AB serum and 10% DMSO at a final concentration of 10×10^6 ml^{-1} and were stored in liquid nitrogen. Subsequently, cryovials were thawed in a 37°C water bath. PBMCs were washed by adding 5 ml of room-temperature, heat-inactivated, filtered human AB serum and then 5 ml of RPMI-1640 + GlutaMAX I + 25 mM HEPES per 10×10^6 cells, in a drop-wise fashion [40]. Finally, $CD4^+$ T cells were obtained from PBMCs by using the Dynabeads Untouched Human CD4 T cells kit and also cell purity was assessed using flow cytometry.

2.8. Biocompatibility test: Cell seeding, viability and spreading of PC12 cells.

PC12 cells were used for evaluation of biocompatibility of electrospun scaffolds. After the crosslinking step, samples (with different ratios of chiotosan and gelatin) were cut to the size of a well from a 24 well plate using a punch. Then, they were sterilized with 70% (v/v) ethanol for 2 h, rinsed three times in double-distilled water, and then immersed in PBS for two days. Before cell seeding, PC12 cells were cultured in 85% RPMI-1640 medium, 5% FBS, and 10% heat-inactivated horse serum. Cells were maintained in a humid, 5% CO_2 incubator and passaged by 0.25% trypsin at 1:2 every other day. Subsequently, prepared electrospun nanofibers were placed in 24-well plate, cells were seeded at a density of 3.6×10^5 cells/ml and cultured in DMEM medium with 1% HS, 0.5% FBS, and 1% antibiotic/antimycotic solution. Also, the blank wells were used as positive controls. The cells were incubated in a humidified incubator at 37°C with 5% CO_2 and then maintained in the incubator for 12 and 72 h. The cell viability and spreading on different electrospun scaffolds was monitored after 12 and 72 h. The cell-scaffold constructs were washed with PBS, fixed in 3% glutaraldehyde for 3 h, washed with DI water, followed by washings with 90% of ethanol. After final washing with 100% ethanol, added with hexamethyldisilazane, air-dried and studied under SEM. The mean number and coverage area of cells cultured on the different samples were quantified by Image ProPlus software (version 3).

2.9. OLN-93 and T-cells seeding: Viability and spreading of OLN-93 cells.

As an *in vitro* model system for MS, the OLN-93cell line (a spontaneously transformed cell line from primary rat brain glial culture) was used [14], frequently used as a model for oligodendrocytes, and T-cell line was obtained from peripheral blood of MS patients and controls as described in this study. Electrospun scaffolds were cut to the size of a well from a 96 well plate. Scaffolds were sterilized with 70% (v/v) ethanol for 2 h, washed three times in double-distilled water and then immersed in PBS for two days. Before cell seeding, OLN-93 cells and T-cells were cultured separately (OLN-93cells: in DMEM supplemented with 10% FBS and T-cells: RPMI-1640 supplemented with 10% FBS, penicillin, and streptomycin). Then, scaffolds were placed in 96-well plate, 4×10^5 OLN-93 cells and 2.8×10^5 T-cells were seeded in a 96-well plate, cultured in DMEM medium supplemented with 10% heat-inactivated fetal calf serum (FCS), 50 U/ml penicillin and 50 µg/ml streptomycin and were maintained for 24 and 72 h in the incubator at 37°C, 5% CO_2. The cell viability and morphology were monitored using SEM and light microscopy as described for PC12 cells in previous method in this study.

2.10. mRNA analysis of OLN-93 cells.

After 1, 3 and 7 day(s) of incubation, total RNA was isolated from cultured cells on nanofiberous scaffolds with TRIzol reagent according to the manufacturer's instructions. mRNA was purified from total RNA using the Poly(A)-Tract mRNA isolation system. Single-strand cDNA was obtained via reverse transcription using 1 µg of total RNA [41]. The prepared cDNA was used for real time quantitative polymerase chain reaction (rt-qPCR) amplification with proper primers. Oligo primer analysis software was applied for designing and choosing primers for real-time PCR analysis (Table 2.). Differential expression of B7-1 (CD80), B7-2(CD86), and IL-12p40 were determined using real-time PCR analysis by iQ5 real-time PCR machine.

Table2. The sequence of cytokine primers used for PCR.

Cytokine	Forward Primer	Reverse Primer
B7-1	5'-GTC CAA ATT GTT GGC TTT CA-3'	5'-GAA GAA TGC CTC ATG ATC CC-3'
B7-2	5'-TGA TTC GGA CAG TTG GAC CCT GAG AC-3'	5'-AAG GTG AAG ATA AAA GCC GC-3'
IL-12p40	5'-CCA AGA ACT TGC AGC TGA AG-3'	5'-TGG GTC TAT TCC GTT GTG TC-3'

3. RESULTS SECTION

3.1. Electrospun nanofiberous scaffolds.

Figure 1 showed SEM micrographs of the electrospun chitosan and gelatin nanofibers (voltage: 12 kV, flow rate: 0.1 ml/h, and distance: 16 cm). Mats were electrospun from chitosan and gelatin with volume ratios of chitosan/gelatin 80:20, 50:50, and 20:80. These micrographs showed that the ratio of chitosan and gelatin had influence on the fiber diameters of fabricated nanofibers.

Figure 1. and Table 3. showed that the effect of ratios of chitosan and gelatin on fibers diameter was studied. By increasing the gelatin ratio in scaffolds, the fiber diameters were increased from 170±73 to 410±175. These values showed that fabricated scaffolds were suitable for neural tissue engineering applications [42]. Also, any further reduction in the portion of gelatin (<20%) caused significant bead formation. Hence, gelatin could improve the ability of chitosan fiber-forming, and the fabricated nanofibers became smoother. In addition, the contact angles and porosity of electrospun scaffolds are shown in Table 3.

The contact angles of the scaffold are directly related to hydrophilicity [43]. The hydrophilicity of electrospun nanofiberous scaffolds could play an important role in the cell

adhesion and proliferation behavior. Scaffolds with higher hydrophilicity are more desirable for cell-growth [18].

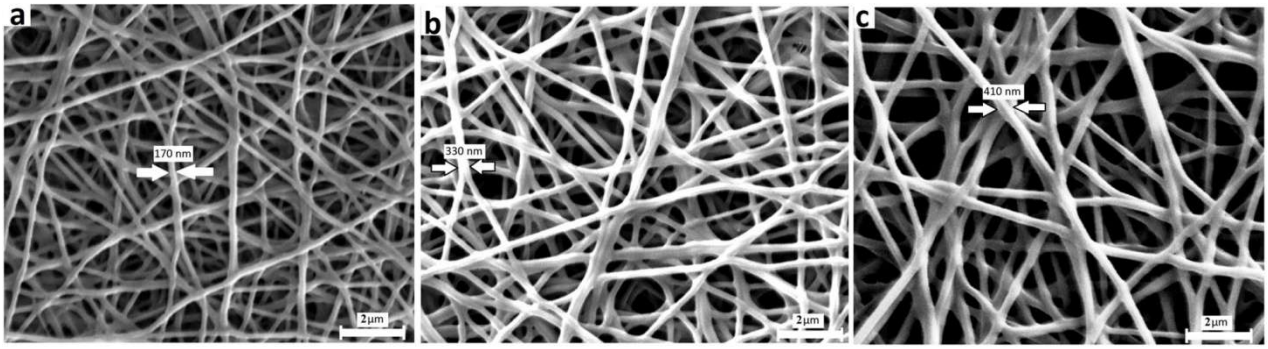

Figure 1. Scanning electron micrographs (a, b and c) of electrospun chitosan and gelatin complex nanofibers. Chitosan/gelatin ratio: (a) 80:20, (b) 50:50 and (c) 20:80. (Flow rate: 0.1 mL/h, voltage: 12 kV and distance between nozzle and collector: 16 cm).

Table 3. Fiber diameter, porosity and contact angle for chitosan and gelatin electrospun scaffolds with different ratio.

Scaffolds (v/v)	Fiber Diameter(nm)	Porosity (%)	Contact angle (°)
Chitosan/Gelatin 20:80	410 ± 175	87 ± 2	68 ± 3
Chitosan/Gelatin 50:50	330 ± 105	85 ± 3	72 ± 2
Chitosan/Gelatin 80:20	170 ± 73	81 ± 4	76 ± 3

Also, a highly porous structure is favorable to make possible cell seeding or migration throughout the material and porosity plays a vital role in cell attachment and the exchange of nutrient and metabolic waste. The porosity and contact angle of the electrospun nanofiberous scaffolds were 81 to 87% and 68 to 76°, respectively, showing that the structures were highly porous and hydrophile. These results indicated that the ratios of chitosan and gelatin (in the range of 20 to 80%) had little or no effect on the hydrophilicity and porosity of nanofiberous scaffold. Wettability of chitosan was changed by blending with gelatin, but the contact angles for all the materials were less than 76°, showing that all materials had good hydrophilicity. Also, due to the fact that the surface hydrophobicity of all the scaffolds was comparable, the cell proliferations cannot be dependent on these factors alone.

3.2. Biocompatibility of scaffolds: Cell viability, spreading and morphology of PC12 cells.

Biocompatibility test of scaffolds has been carried out using PC12 cells. Cell morphology can be affected by the substrate that a cell is attached to. Therefore, cell morphology is a significant characteristic in tissue engineering scaffold. The cell morphology is influenced not only by chemical factors, but also by substrate topography. In this work, cells demonstrated different characteristics onto the different substrate. Here, the result of morphological features and viability of PC12 cells after 72 h onto electrospun scaffolds with different ratios of chitosan and gelatin are as shown in Figure 2. The morphology of PC12 cells attached on nanofiberous scaffolds and the contacts between cells and scaffolds were subjected to SEM investigation after culture for 3 days. As shown in Figure 2, the PC12 cells appeared spindle shaped on 80:20 and 20:80 chitosan and gelatin nanofibers (a' and c') and the cell morphology on nanofibers with equal ratio of chitosan and gelatin (b') had a high spreading level that was more than other scaffolds.

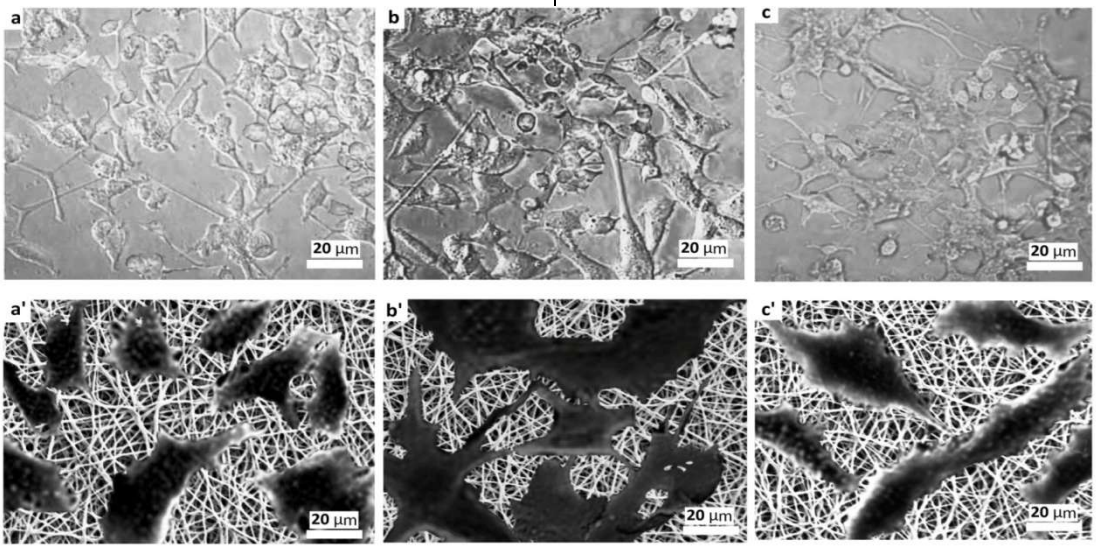

Figure 2. SEM images, Morphological features and viability of PC-12 cells after 72 hours onto: electrospun chitosan and gelatin nanofiberous scaffolds. Chitosan/gelatin ratio: (a, a') 80:20, (b, b') 50:50 and (c, c') 20:80.

Also, as shown in Figures 3 and 4, the value of cell spreading and cell number determined after 12 and 72 h on to the different scaffolds and control.

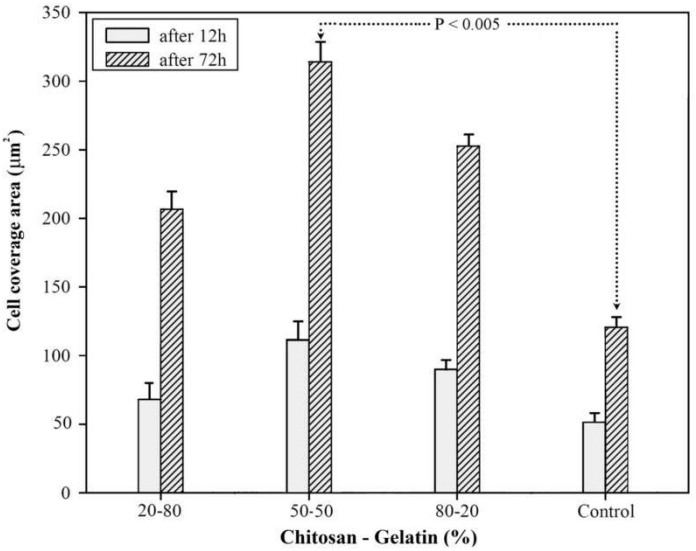

Figure 3. The effect of different ratio of chitosan and gelatin in the electrospun scaffolds on PC-12 cell coverage area. Control: cell culture plate. Data are expressed as means ± SD, n=8.

The results of these two tests were highly notable, because the results of cell spreading assay were similar to cell number assay. It means that similar to the results of SEM and light microscopy analysis (Figure 2), higher and lower cell spreading and cell number were observed on electrospun scaffold with an equal ratio of chitosan and gelatin (50:50) and control (cell culture plate), respectively (Figures 3 and 4). This fact showed that nanofibers with 50% chitosan and 50% gelatin are ideal option for neural tissue engineering. Thus, cells were grown on electrospun mixtures of chitosan and gelatin and considered optimal for use in nerve regeneration. Gelatin interacts strongly with chitosan forming polyelectrolyte complexes and makes the surface more hydrophilic, because gelatin is an anionic molecule used to modify chitosan [27]. It makes the chitosan and gelatin blends more adhesives in promoting optimal differentiation of PC12 cells at equal mixing ratio [27].

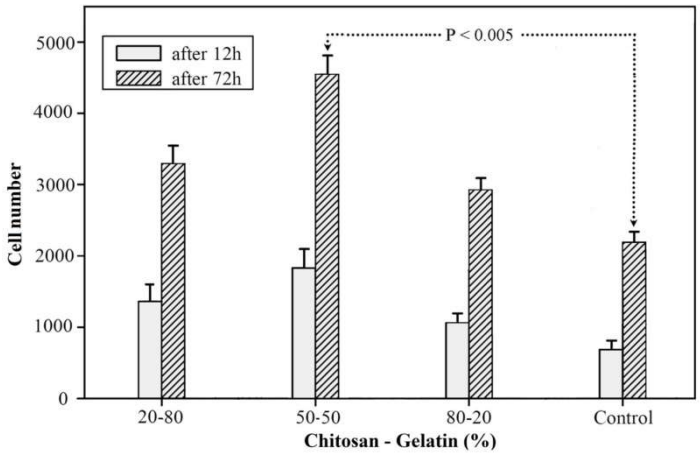

Figure 4. The effect of different ratio of chitosan and gelatin in the electrospun scaffolds on PC-12 cell number. Control: cell culture plate. Data are expressed as means ± SD, n=8.

This interaction was shown to be proven to be profitable for neurons. Also, according to this result, other scaffolds (80:20 and 20:80) had a significant positive effect on PC12 cell morphology in comparison with controls and these are suitable for applications in nervous systems. Totally, proliferation of PC12 cells on nanofibers showed that fabricated nanofibers are non-toxic and highly biocompatible for neural tissue engineering applications.

3.3. OLN-93 and T-cells seeding cell viability, spreading and morphology of OLN-93 cells.

An *in vitro* environment for modeling MS and investigate the effects of T-cells on OLN-93 cells morphology and viability was fabricated in this aspect of the study. Morphological features and viability of OLN-93 cells after 24 and 72 h on to nanofiberous scaffolds and control (in the presence and absence of T-Cells of subjects) are as shown in Figure 5. As shown in SEM micrograph in Figure 5A, OLN-93 and T-cells adhered well to nanofibers in the first hour after seeding. In fact, nanofibers were applied as a proper environment like a natural ECM for cell attachment and proliferation. In addition, it is known that strong adhesion of the cells to the substrate is essential for an adequate cell proliferation [20-22]. Interestingly, the image obtained from light microscopy (Figure 5B) and quantified proliferation of adherent OLN-93 cells after 24 and 72 h of incubation post-seeding in Figure 5C, demonstrated that the proliferation and spreading of cells on nanofiberous scaffold (in the absence of T-Cell) (sample a) was significantly higher when compared with the control (sample b) and other samples.

For the first time, our data demonstrated that the chitosan and gelatin nanofibers are a biocompatible scaffold for oligodendrocytes proliferation. Additionally, our study elucidated the hurdles in understanding the differences in reduction of glial scaring between two different substrates (Nanofibers vs. flat substrates) [44, 45]. When oligodendrocytes cultured in the presence of T-cells of MS patients (samples c and e), the cells number was severely decreased. The findings of this study once again provided the fact that autoreactive T-cells attack on oligodendrocytes is an important event in progression of disease in MS patients [3]. Although, the decreasing effects of T-cell of the controls on oligodendrocytes number (samples d and f) was not in the level of effects of T-cell of MS patients (as expected); results showed that this cells had a negative influence on oligodendrocyte proliferation. We think that the main reason for this event can directly be related to change in activity of T-cells within experiments, such as T-cells isolation from peripheral blood and T-cell line generation procedures.

3.4 mRNA analysis of OLN-93 cells.

mRNA expression levels (average) of B7-1, B7-2, and IL-12p40 in OLN-93 seeded on different substrates in the presence and absence of the T-cells of controls and MS patients are shown in Figure 6. Our results demonstrated that mRNA expression of these genes in OLN-93 cells seeded on electrospun chitosan and gelatin scaffold in co-culture of autoreactive T cells of MS patients (sample c) was significantly greater than other samples. Herein, for the first time, the up regulation of stimulatory markers in OLN-93 cells was demonstrated as the direct effect of aggressive autoreactive T cells [3] (in comparison with samples a,

b, d and f). More importantly, the morphology and topography of nanofiberous scaffold, [46] resulted in the larger cell areas and subsequently, the increased cell surface area improve the cell attachment and cause internalization of nucleic acid complexes [47] (in comparison with samples b, e and f).

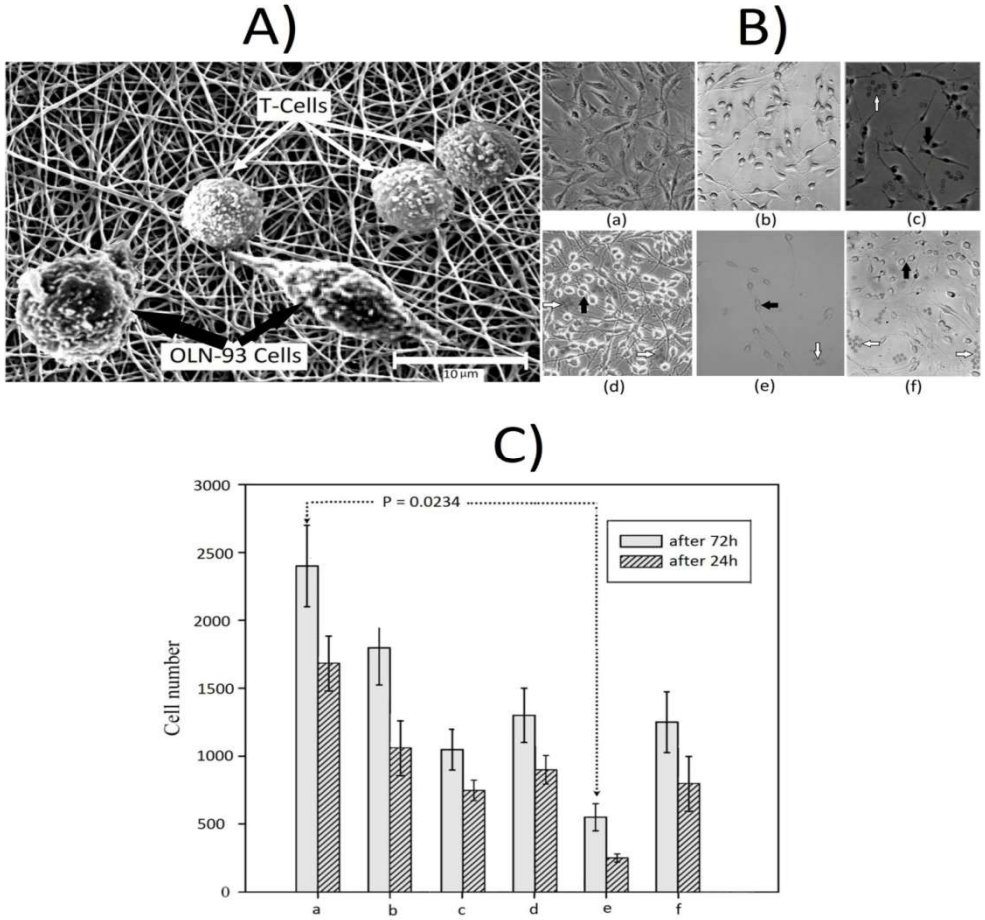

Figure 5. (A) SEM images of OLN-93 and T-Cells after 1 hour culture on electrospun chitosan and gelatin scaffold. **(B)** Morphological features and viability of OLN-93 cells after 24 hours onto: (a) electrospun chitosan and gelatin scaffold, (b) control surface (cell culture plate), (c) electrospun chitosan and gelatin scaffold in the presence of the TMP, (d) electrospun chitosan and gelatin scaffold in the presence of the TC, (e) cell culture plate in the presence of the TMP and (f) cell culture plate in the presence of the TC. The OLN-93 and T-cells are marked with black and white arrow respectively.(TMP: T-Cells of multiple sclerosis Patient(isolated from PBMC) and TC: T-Cells of Control subjects(Isolated from PBMC)). **(C)** The effects of culture substrate and also T-cells on OLN-93 cell number in different samples. Data are expressed as means ± SD, n=8.

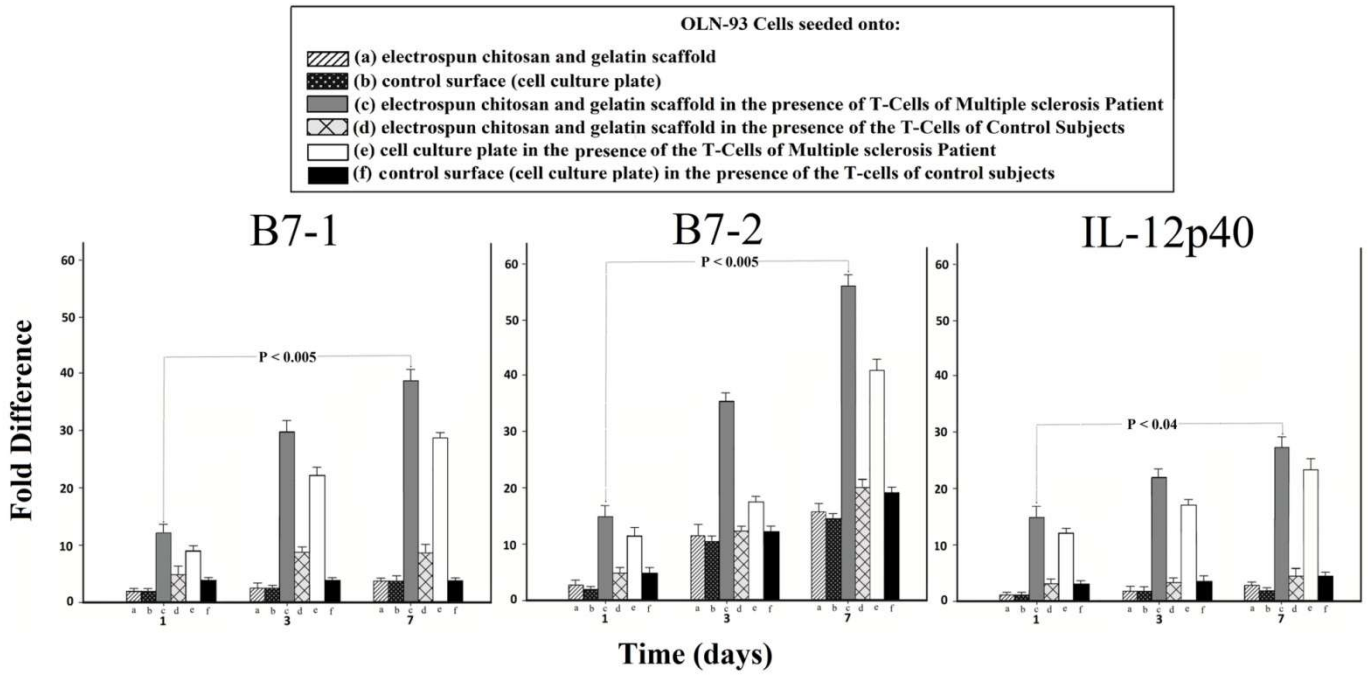

Figure 6. mRNA expression levels (average) of B7-1, B7-2 and IL-12p40 for OLN-93 seeded on different substrate in (or without) the presence of the T-cells of controls and multiple sclerosis patients. Data are expressed as means ± SD, n=8.

Also, the increase of B7-1 (CD80), B7-2 (CD86), and IL-12p40 expression verified and completed the result of previous studies in animal models which showed that these molecules are differently involved in T-cell stimulation [48, 49]. This is as a result of the fact that previous results with our results proved the effects of T-cell stimulations and the increase of B7-1(CD80), B7-2 (CD86), and IL-12p40 expression had reciprocal effects on each other. Additionally, the reason of increased gene expression for oligodendrocytes in the presence of T-cells from healthy controls (samples d and f) can correlate with the antigen presenting capacity of T-cells. It is known that autoreactive T-cells are present in the circulation of normal individuals without any pathologic results. Therefore, the increased expressions of these molecules by T-cells from healthy controls were found in relation to antigen presenting capacity of these T-cells. Our finding showed that the sample c (Figure 6.), as an *in vitro* model for MS, can be applied for future studies on MS treatment. These examinations may include etiology of MS, effects of fabricated drug, and its doses before clinical assay and influence of different biomarkers on progress or control of disease.

4. CONCLUSIONS

In this work, crosslinked nanofibers were designed and fabricated which consist of chitosan and gelatin with several weight ratios to mimic natural ECM for neural tissue engineering applications. SEM, contact angle test, porosity measurement, and biocompatibility of mats using PC-12 cells were used to study the properties of scaffolds for neural tissue engineering. Then, an *in vitro* environment consisting of OLN-93 cells, T-cells (obtained from MS patients and healthy controls) and chitosan/gelatin nanofibers for fabricating a simple *in vitro* model for MS were designed. Besides, the assessments of effects of MS patients' T-cells on OLN-93 cells number and morphology onto different substrate were performed to achieve an ideal model through several samples. Finally, mRNA analysis of oligodendrocytes was carried out for the evaluation of B7-1(CD80), B7-2(CD86), and IL-12p40 expressions. Results showed that fabricated nanofibers had an acceptable level of biocompatibility for neural tissue engineering applications. Also, in the seeded OLN-93 cells onto nanofibers in the presence of autoreactive T-cells, the number of oligodendrocytes was significantly decreased and this event can directly be related to T-cells attacking on oligodendrocytes similar to pathological events in MS. The increase of B7-1(CD80), B7-2 (CD86), and IL-12p40 expressions verified the capability of this model for molecular evaluations in MS. Further studies will be focused on the evaluation of fabricated drug and its doses before clinical assay and influence of different biomarkers in this environment.

5. REFERENCES

[1] Lassmann H., Comparative neuropathology of chronic experimental allergic encephalomyelitis and multiple Sclerosis, *Springer-Verlag*, **1983.**

[2] Bhattacharya A., Mishra R., Tiwari P., Multiple sclerosis: an overview, *Asian Pac J Trop Med*, 2, 1954-1962, **2012.**

[3] Stinissen P., Raus J., Zhang J., Autoimmune pathogenesis of multiple sclerosis: role of autoreactive T lymphocytes and new immunotherapeutic strategies, *Crit Rev Immunol*, 17, 33-75, **1997.**

[4] Ziemann U., Wahl M., Hattingen E., Tumani H., Development of biomarkers for multiple sclerosis as a neurodegenerative disorder, *Prog Neurobiol,* 95, 670-685, **2011.**

[5] D'Ambrosio A., Pontecorvo S., Colasanti T., Zamboni S., Francia A., Margutti P., Peripheral blood biomarkers in multiple sclerosis, *Autoimmun Rev*, 14, 1097-1110, **2015.**

[6] McArthur J.G., Raulet D,H., CD28-induced costimulation of T helper type 2 cells mediated by induction of responsiveness to interleukin 4, *J Exp Med*, 178, 1645-1653, **1993.**

[7] Linsley P.S., Ledbetter J.A., The role of the CD28 receptor during T cell responses to antigen, *Annu Rev Immunol*, 11, 191-212, **1993.**

[8] Hofman F.M., Hinton D.R., Johnson K., Merrill J.E., Tumor necrosis factor identified in multiple sclerosis brain, *J Exp Med*, 170, 607-612, **1989.**

[9] Sharief M.K., Hentges R., Association between tumor necrosis factor alpha and disease progession in patients with multiple sclerosis, *New Engl J Med*, 325, 467-472, **1991.**

[10] Woodroofe M.N., Cuzner M.L., Cytokine mRNA expression in inflammatory multiple sclerosis lesions: detection by non-radioactive in situ hybridization, *Cytokine*, 5, 583-588, **1993.**

[11] Correale J., McMillan M., Li S., McCarthy K., Le T., Weiner L.P., Antigen presentation by autoreactive proteolipid protein peptide specific T cell clones from chronic progressive multiple sclerosis patients: roles of costimulatory B7 molecules and IL-12, *J Neuroimmunol*, 72, 27–43, **1997.**

[12] Thompson C.B., Distinct roles for costimulatory ligands B7-1 and B7-2 in T helper cell differentiation, *Cell*, 81, 979–982, **1995.**

[13] De Vries G.H., Boullerne A.I., Glial cell lines: an overview, *Neurochem Res*, 35, 1978-2000, **2010.**

[14] Richter-Landsberg C., Heinrich M., OLN-93: A new permanent oligodendroglia cell line derived from primary rat brain glial cultures, *J Neurosci Res*, 45, 161-173, **1996.**

[15] Wang X., Lin P., Yao Q., Chen C., Development of small-diameter vascular grafts, *World J Surg*, 31, 682-689, **2007.**

[16] Mooney D.J., Mikos A.G., Growing new organs, *Sci Am*, 280, 60-65, **1999.**

[17] Griffith L.G., Naughton G., Tissue engineering current challenges and expanding opportunities, *Science*, 295, 1009-1014, **2002.**

[18] Langer R., Vacanti J.P., Tissue engineering, *Science*, 260, 920-926, **1993.**

[19] Qian Y.F., Zhang K.H., Chen F., Ke Q.F., Mo X.M., Cross-linking of gelatin and chitosan complex nanofibers for tissue engineering scaffolds, *J Biomat Sci-Polym E*, 22, 1099–1113, **2011.**

[20] Xu C.Y., Inai R., Kotaki M., Ramakrishna S., Aligned biodegradable nanofibrous structure: a potential scaffold for blood vessel engineering, *Biomaterials*, 25, 877-886, **2004.**

[21] Ma Z., Kotaki M., Inai R., Ramakrishna S., Potential of nanofiber matrix as tissue engineering scaffolds, *Tissue Eng*, 11, 101-109, **2005.**

[22] Smith L.A., Ma P.X., Nano-fibrous scaffolds for tissue engineering, *Colloid Surface B*, 39, 125-131, **2004.**

[23] Aluigi A., Varesano A., Montarsolo A., Vineis C., Ferrero F., Mazzuchetti G., Tonin C., Electrospinning of Keratin/poly (ethylene oxide) blend nanofibers*, JAppl Polym Sci*, 104, 863-870, **2007.**

[24] Bellan L.M., Craighead H.G., Control of an electrospinning jet using electric focusing and jet-steering fields, *J Vac Sci Technol B*, 24, 3179-3183, **2006.**

[25] Alli A., Hazer B., Menceloglu Y., Suzer E., Synthesis, Characterization and surface properties of amphiphilic polystyrene-b-polypropylene glycol block copolymers, *Eur Polym J*, 42, 740-750, **2006.**

[26] Haipeng G., Yinghui Z., Jianchun L., Yandao G., Nanming Z., Xiufang Z., Studies on nerve cell affinity of chitosan-derived materials, *J Biomed Mater Res*, 52, 285–295, **2000.**

[27] Cheng M., Deng J., Yang F., Gong Y., Zhao N., Zhang X., Study on physical properties and nerve cell affinity of composite films from chitosan and gelatin solutions, *Biomaterials*, 24, 2871–2880, **2003.**

[28] Cheng M., Cao W., Gao Y., Gong Y., Zhao N., Zhang X., Studies on nerve cell affinity of biodegradable modified chitosan films, *J Biomat Sci-Polym E*, 14, 1155–1167, **2003.**
[29] Mingyu C., Kai G., Jiamou L., Yandao G., Nanming Z., Xiufang Z., Surface modification and characterization of chitosan film blended with poly-l-lysine, *J Biomater Appl*, 19, 59–75, **2004.**
[30] Li X., Yang Z., Zhang A., Wang T., Chen W., Repair of thoracic spinal cord injury by chitosan tube implantation in adult rats, *Biomaterials*, 30, 1121–1132, **2009.**
[31] Lu G.Y., Kong L.J., Sheng B.Y., Wang G., Gong Y.D., Zhang XF., Degradation of covalently crosslinked carboxymethyl chitosan and its potential application for peripheral nerve regeneration, *Eur Polym J*, 43, 3807–3818, **2007.**
[32] Wang G., Lu G.Y., Ao Q., Gong Y.D., Zhang X.F., Preparation of cross-linked carboxymethyl chitosan for repairing sciatic nerve injury in rats, *Biotechnol Lett*, 32, 59–66, **2010.**
[33] Freier T., Koh H.S., Kazazian K., Shoichet M.S., Controlling cell adhesion and degradation of chitosan films by N-acetylation, *Biomaterials*, 26, 5872–5878, **2005.**
[34] Yang Y., Liu M., Gu Y., Lin S., Ding F., Gu X., Effect of chitooligosaccharide on neuronal differentiation of PC-12 cells, *Cell Biol Int*, 33, 352–356, **2009.**
[35] Onishi H., Machida Y., Biodegradation and distribution of water-soluble chitosan in Mice, *Biomaterials*, 20, 175–182, **2009.**
[36] Li Q., Dunn E.T., Grandmaison E.W., Goosen M.F.A., Applications and properties of chitosan, *J Bioact Compat Pol*, 71, 370–397, ***1*992.**
[37] Huang Z.M., Zhang Y.Z., Kotaki M., Ramakrishna S., A review on polymer nanofibers by electrospinning and their applications in nanocomposites, *Compos Sci Technol*, 63, 2223–2253, **2003.**
[38] Park W.H., Jeong L., Yoo D.I., Hudson S., Effect of chitosan on morphology and conformation of electrospun silk fibroin nanofibers, *Polymer*, 45, 7151–7157, **2004.**
[39] Tree T.I., Roep B.O., Peakman M., Enhancing the sensitivity of assays to detect T cell reactivity: The effect of cell separation and cryopreservation media, *Ann NY Acad Sci*, 1037, 26–32, **2004.**
[40] Dendrou C.A., Plagnol V., Fung E., Yang J.H.M., Downes K., Cooper J.D., Nutland S., Coleman G., Himsworth M., Hardy M., Burren O., Healy B., Walker N.M., Koch K., Ouwehand W.H., Bradley J.R., Wareham N.J., Todd J.A. and Wicker L.S., Cell-specific protein phenotypes for the autoimmune locus IL2RA using a genotype selectable human bioresource, *Nat Genet*, 41, 1011-1015, **2009.**
[41] Choi D.J., Choi S.M., Kang H.Y., Min H.J., Lee R., Ikram M., Subhan F., Jin S.W., Jeong Y.H., Kwak J.Y., Yoon S., Bioactive fish collagen/polycaprolactone composite nanofibrousscaffolds fabricated by electrospinning for 3D cell culture, *Res J Biotechnol*, 205, 47-58, **2015.**
[42] Cao H., Liu T., Chew S.Y., The application of nanofibrous scaffolds in neural tissue engineering, *Adv Drug Deliver Rev*, 61, 1055–1064, **2009.**
[43] Johnson R.E., Dettre R.H., Surface and Colloid Science, *Wiley*, **1969.**
[44] McKeon R.J., Schreiber R.C., Rudge J.S., Silver J., Neurosci J., Reduction of neurite outgrowth in a model of glial scarring following CNS injury is correlated with the expression of inhibitory molecules on reactive astrocytes, *J Neurosci,* 11, 3398-3411, **1991.**
[45] Nisbet D.R, Rodda A.E., Horne M.K., Forsythe J.S., Finkelstein D.I., Neurite infiltration and cellular response to electrospun polycaprolactone scaffolds implanted into the brain, *Biomaterials*, 30, 4573-4580, **2009.**
[46] Cao H., Marcy G., Goh E.L.K., Wang F., Wang J., Chew S.Y., The effects of nanofiber topography on astrocyte behavior and gene silencing efficiency, *Macromol Biosci*, 12, 666–674, **2012.**
[47] Adler A.F., Leong K.W., Emerging links between surface nanotechnology and endocytosis: impact on nonviral gene delivery, *Nano Today*, 5, 553-569, **2010.**
[48] Windhagen A., Newcombe J., Dangond F., Strand C., Woodroofe M.N., Cuzner M.L., Hafler D.A., Expression of costimulatory molecules B7-1 (CD80), B7-2 (CD86), and interleukin 12 cytokine in multiple sclerosis lesions, *J Exp Med*, 182, 1985-1996, **1995.**
[49] Monteyne P., Guillaume B., Sindic C.J., B7-1(CD80), B7-2(CD86), interleukin-12 and transforming growth factor-β mRNA expression in CSF and peripheral blood mononuclear cells from multiple sclerosis patients, *J Neuroimmunol*, 91, 198–203, **1998.**

6. ACKNOWLEDGEMENTS

The authors would like to thank Ms. Pegah Mehrpouya-Bahrami and Dr. Mojtaba Ansari for their technical assistance, valuable suggestions and encouragement throughout this work.